

RSC Advances



This is an *Accepted Manuscript*, which has been through the Royal Society of Chemistry peer review process and has been accepted for publication.

Accepted Manuscripts are published online shortly after acceptance, before technical editing, formatting and proof reading. Using this free service, authors can make their results available to the community, in citable form, before we publish the edited article. This *Accepted Manuscript* will be replaced by the edited, formatted and paginated article as soon as this is available.

You can find more information about *Accepted Manuscripts* in the [Information for Authors](#).

Please note that technical editing may introduce minor changes to the text and/or graphics, which may alter content. The journal's standard [Terms & Conditions](#) and the [Ethical guidelines](#) still apply. In no event shall the Royal Society of Chemistry be held responsible for any errors or omissions in this *Accepted Manuscript* or any consequences arising from the use of any information it contains.

Cite this: DOI: 10.1039/c0xx00000x

www.rsc.org/xxxxxx

ARTICLE TYPE

Reduction degree and property study of graphene nanosheets prepared with different reducing agents and their applicability of being a carrier of Ru(phen)₃Cl₂ luminescent sensor for DNA detection

Hongjuan Li, Jia Wen, Ruijin Yu, Caihui Bai, Yongqian Xu, Shiguo Sun*

5 Received (in XXX, XXX) Xth XXXXXXXXX 20XX, Accepted Xth XXXXXXXXX 20XX
DOI: 10.1039/b000000x

Recently, graphene nanosheets (GNS) have been widely investigated and used in capacitors, catalysts, biological/chemical sensors, etc. However, the feasible applications of GNS prepared with different reducing agents as a carrier of luminescent sensor have never been systematically studied yet. Herein, a serial of GNS were acquired using different reducing agents, such as hydrazine, glucose and urea. The reduction degrees and properties of the GNS samples were systematically studied by using X-ray diffractometer, Raman spectra, IR spectra and X-ray photoelectron spectroscopy. The results indicated that the reduction degree was in the order of hydrazine>glucose>urea, demonstrating that reducing agents plays an important role in the bulk fabrication of high quality graphene. Then the GNS samples were all employed as a carrier of Ru(phen)₃Cl₂ (tris(1,10-phenanthroline)ruthenium(II) dichloride) sensor to discriminate DNA. It is found that all the GNS samples can effectively quench the emission of the Ru(phen)₃Cl₂ sensor. After addition of a certain amount of DNA into the corresponding systems, the luminescence intensity was all fully recovered. By comparison, the luminescence response of GNS-G prepared with glucose shows the best linear correlation to the DNA added, with a detection limit of 3.62×10⁻⁹ g/mL, indicating GNS-G can be employed as a good carrier of Ru(phen)₃Cl₂ to discriminate DNA. This work will significantly advance the research of bulk fabrication of high quality graphene and the specific applications in luminescent sensor of the graphene-based functional materials in the future.

Introduction

In recent years, graphene nanosheets (GNS) have attracted widely attention due to their large specific surface area, good biocompatibility, unique electrical/thermal characteristics, etc.¹⁻⁵ Owing to their unique nanostructure and excellent properties, GNS have shown potential applications in the field of capacitors, catalysts, biological/chemical sensors, cellular imaging, drug delivery, and so on.⁶⁻¹⁰

At present, chemical reduction of exfoliated graphite oxide (GO) is considered as an efficient approach to produce GNS due to its low cost, economic feasibility and massive scalability.¹¹⁻¹³ And the chemical reduction was usually carried out using hydrazine, glucose and urea as the reducing agent.¹⁴⁻¹⁶ However, to our knowledge, the feasible applications of GNS prepared with different reducing agents as a carrier of luminescent sensor have never been systematically studied yet.

Reduced GNS is composed of sp² hybridized carbon atoms arranged in a honeycomb lattice with different types of oxygen-containing functional groups: carbonyl, carboxylate and epoxy groups on the basal planes.¹⁷ Because GNS is negatively charged, it can immobilize positive charged materials through both electrostatic and π-π stacking interaction.¹⁸ Previous research has shown that carbon materials can be served as effective fluorescent sensing platforms for nucleic acid detection.¹⁹⁻²³ GNS can

effectively quench the luminescence of dye through π-π stacking and electrostatic interaction.²⁴⁻²⁵ For instance, Ru(phen)₃Cl₂ (tris(1,10-phenanthroline)ruthenium(II) dichloride) is one type of good candidate due to the co-existing of the positive charged Ru atom and the aromatic rings of phen (the structure is shown in Supporting information Figure S1). Especially, Ru(phen)₃Cl₂ is the suitable candidate for deoxyribonucleic acid (DNA) site-specific, it can bind DNA by partial interaction and shows a strong preference for poly[d(A-T)] to poly[d(C-G)].²⁶⁻²⁸ After being encountered with DNA, Ru(phen)₃Cl₂ can be released from GNS and interacted with CT DNA immediately, leading to a luminescence recovery of Ru(phen)₃Cl₂. Based on this, a GO-Ru(phen)₃Cl₂ fluorescence material exhibiting enhanced properties was developed to image both fixed cells and live cells.²⁹

Inspired by this, herein, a serial of GNS were fabricated using different reducing agents, such as hydrazine, glucose and urea. The reduction degrees and properties of the obtained GNS samples were systematically investigated by XRD, Raman spectra, IR spectra and XPS analysis. Then the feasible applications of GNS prepared with different reducing agents as a carrier of luminescent sensor have been systematically studied. It is found that all the GNS samples can effectively quench the emission of the Ru(phen)₃Cl₂ sensor. After addition of a certain

amount of DNA into the corresponding systems, the luminescence intensity was all fully recovered. By comparison, the luminescence response of GNS-G prepared with glucose shows the best linear correlation to the DNA added, indicating GNS-G can be employed as a good carrier of Ru(phen)₃Cl₂ to discriminate DNA.

Experimental

Materials

All the chemicals are of analytical grade and were used without further purification. Natural flake graphite (325 mesh) was purchased from Alfa-Aesar Co. Calf thymus DNA (CT DNA) was purchased from Sigma Chemical Co. Ultrapure Milli-Q water ($\rho > 18.0 \text{ M}\Omega \text{ cm}$) was used throughout the luminescence experiments. Ru(phen)₃Cl₂ used in experiments were synthesized according to the literature procedure.³⁰

Preparation of graphene nanosheets with different reducing agents

Graphite oxide (GO) was synthesized from natural flake graphite by a modified Hummers method.³¹ The as-prepared GO was dispersed in ultrapure water and sonicated for 60 min to achieve the exfoliation of GO dispersion (0.2 mg/mL) for further use. Then, a serial of graphene nanosheets (GNS) were acquired using different reducing agents, such as hydrazine, glucose and urea, which were abbreviated as GNS-H, GNS-G and GNS-U, respectively.

GNS-H was made followed the literature procedure.¹⁴ In short, 1.4 mL of ammonia solution (25%, w/w) and 0.2 mL of hydrazine solution (25%, w/w) were added to 500 mL of the as-prepared exfoliation GO dispersion (0.2 mg/mL). After being vigorously shaken for 10 minutes, the suspension was then refluxed at 95 °C for 1 h under continuous magnetic stirring. The resulting dispersion was obtained, which was abbreviated as GNS-H.

GNS-U was made followed the literature procedure.¹⁵ In short, 1.0500 g of urea was added to 500 mL of the exfoliation GO dispersion (0.2 mg/mL). After being vigorously shaken for a few minutes, the suspension was then refluxed at 100 °C for 24 h under continuous magnetic stirring. The resulting dispersion was obtained and abbreviated as GNS-U.

GNS-G was made followed the literature procedure.¹⁶ In short, 1.6000 g of glucose was added to 500 mL of the exfoliation GO dispersion (0.2 mg/mL). Then 2.8 mL of aqueous ammonia solution (25%, w/w) was added to the resulting dispersion. After being vigorously shaken for a few minutes, the suspension was then refluxed at 95 °C for 1 h under continuous magnetic stirring. The resulting stable dispersion was obtained and abbreviated as GNS-G.

Characterization

X-ray diffraction (XRD) analysis was carried out with a D/Max2550VB+PC X-ray diffractometer with Cu K α ($\lambda = 0.15406 \text{ nm}$), using an operation voltage and current of 40 kV and 30 mA, respectively. The atomic force microscopy (AFM) image of the synthesized GNS samples deposited on a freshly cleaved mica surface was taken with NanoScope V in tapping mode. Transmission electron microscopy (TEM) images were

collected using a JEM-2100 microscope working at 200 kV. Specimens for observation were prepared by dispersing the samples into alcohol by ultrasonic treatment and dropped on carbon-copper grids. The X-ray photoelectron spectroscopy (XPS) measurement was performed with an Axis Ultra, kratos (UK) spectrometer using Al K α excitation radiation (1486 eV). The Raman spectra were taken at room temperature in the spectra range 400–4000 cm⁻¹ using an ALMEGA-TM Raman spectrometer system. The spectra were recorded using a 532 nm argon ion laser. Fourier transform infrared (FT-IR) spectra were obtained on a Bruker EQUINX55 FT-IR spectrophotometer by a standard KBr disk method in the range 400–4000 cm⁻¹. Specimens for observation were prepared by dispersing the samples into alcohol by ultrasonic treatment and dropped on carbon-copper grids. The absorption and emission spectra were collected using a Shimadzu 1750 UV-visible spectrometer and a RF-5301 fluorescence spectrometer (Japan), respectively.

Luminescence experiments

Stock solution of CT DNA solution ($6.72 \times 10^{-4} \text{ g/mL}$) was prepared by dissolving commercial CT DNA in ultrapure water. Stock solution of Ru(phen)₃Cl₂ (0.49 μM) was prepared in ultrapure water. Then the as-prepared GNS suspension (0.2 mg/mL) was gradually added into Ru(phen)₃Cl₂ solution (3 mL) with stirring until the luminescence was almost quenched. Finally, an increasing amount of CT DNA solution was added until the highest luminescence intensity was reached. The sample was stirred for 5 s each time before the luminescence spectra were recorded. In all the titration experiments, the total volume was maintained not exceed 5% of the original volume.

Results and discussion

X-ray diffraction and morphology analysis

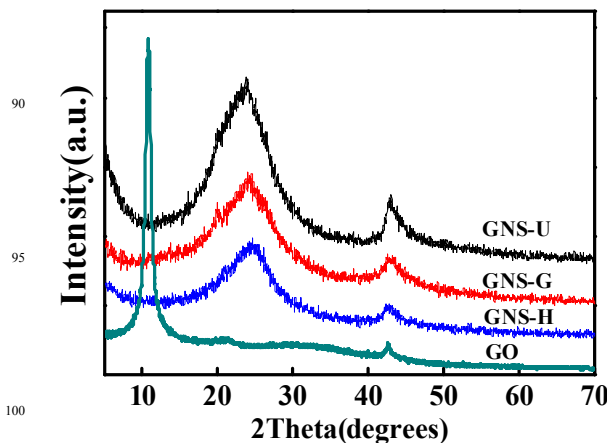


Fig.1 XRD patterns of GO, GNS-U, GNS-G and GNS-H.

The X-ray diffraction (XRD) patterns of GO, GNS-H, GNS-U and GNS-G are presented in Fig. 1. The as-prepared GO has a layered structure with a basal spacing of 0.82 nm, showing the complete oxidation of graphite into the graphite oxide.³² After reduction using different reducing agents, such as hydrazine, glucose and urea, the peak at 10.7° of GO completely disappears, and the obtained GNS samples all shows broad characteristics peak in range of 20~30°, which is corresponded to the (002)

diffraction of graphene.³³ The result suggests that the GO was all reduced to graphene after by treating with different reducing agents.

The morphology of the as-prepared GNS samples was observed by TEM as shown in Fig.2. It is seen that the obtained GNS samples all show the thin nanoplatelets shape with corrugation and scrolling image, which is consistent with the literature.^{34, 35} The thickness of the GNS samples was further characterized by AFM analysis. The results indicated that the average thickness of the GNS-U, GNS-G and GNS-H is about 1.46 nm, 1.39 and 1.34nm, respectively.^{16, 35}

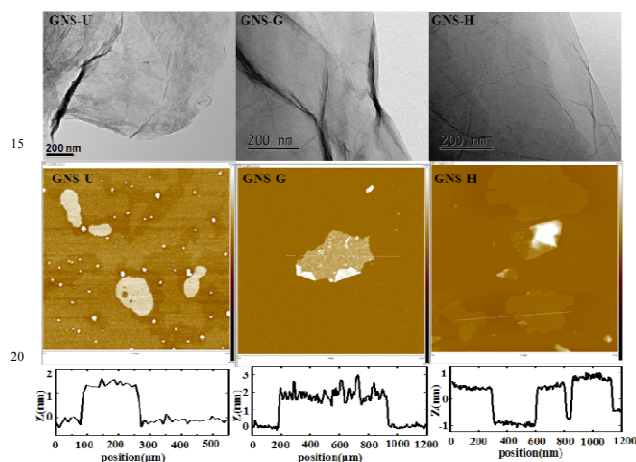


Fig.2 TEM and AFM images of GNS-U, GNS-G and GNS-H. And height profiles along the lines are shown in AFM images.

The effective reduction of GO to GNS can be further demonstrated by the Raman technology. The Raman spectra of GO, GNS-H, GNS-U and GNS-G in the range from 1000 to 3000 cm^{-1} are shown in Fig. 3. The Raman spectrum of GO exhibits a weak D band at around 1361 cm^{-1} and a stronger G band at 1589 cm^{-1} . In general, the G mode ($\sim 1589 \text{ cm}^{-1}$) is assigned to the E_{2g} phonon of sp^2 C atoms. While the D mode ($\sim 1361 \text{ cm}^{-1}$) is arisen from a breathing mode of κ -point phonons of A_{1g} symmetry, which is a common feature of sp^3 defects in carbon and usually can be associated with the structural defects, amorphous carbon, or edges that break the symmetry and selection rule.³⁶⁻³⁷ The I_D/I_G intensity ratio is a measure of the disorder/defects in graphene and average size of the sp^2 domains in graphite materials.³⁸ After reduction with hydrazine and glucose, the D band of the obtained GNS-H and GNS-G samples become prominent. The I_D/I_G intensity ratio for the samples of GNS-H, GNS-U and GNS-G is determined to be 1.31, 0.91 and 1.00, much higher than that of the pristine GO (0.76). The larger I_D/I_G value of the GNS samples prepared with different reducing agents indicates the significant decrease of the average size (or more amount) of the in-plane sp^2 domains and more sp^3 defects/disorders due to the reduction of GO to GNS.^{16, 39-41} By comparison, GNS-H had the highest I_D/I_G intensity ratio (1.31), indicating the highest degree of reduction. GNS-G was the second, then GNS-U. The relative lower I_D/I_G intensity ratio (0.91) of the GNS-U sample can be assigned to the relative incomplete reduction of the GNS-U as compared to the sample of the GNS-G (1.00) and GNS-H (1.31).

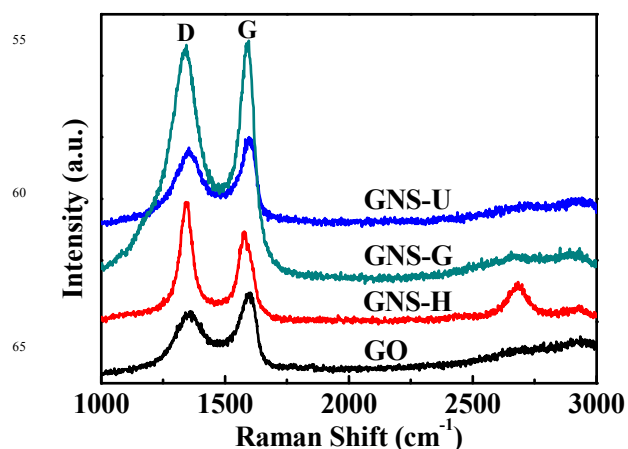


Fig.3 The Raman spectra of GO, GNS-U, GNS-G and GNS-H.

IR spectra analysis

In this study, FTIR spectroscopy was also employed to evaluate the reduction of GO to GNS samples as shown in Fig. 4. The FTIR spectrum of GO exhibits the absorption bands at 3421 cm^{-1} (O-H stretching vibrations), 1717 cm^{-1} (C=O stretching vibrations from carbonyl and carboxylic groups), and 1617 cm^{-1} (C=C stretching vibrations). And the absorption bands at 1300~1000 cm^{-1} correspond to C-O stretching vibrations.⁴²⁻⁴³ After the reduction with hydrazine, urea and glucose, the absorption bands of GNS samples corresponding to oxygen functional groups C-O, and C=O stretching vibrations were decreased significantly, indicating that most of oxygen functional groups on the GO nanosheets are removed.⁴⁴ By comparison, for the sample of GNS-H, the absorption band at 1717 cm^{-1} ($\nu_{C=O}$) was indistinguishable, suggesting that the reduction effect with hydrazine was superior to that with glucose and urea. The IR spectra results are consistent with the Raman spectra analysis.

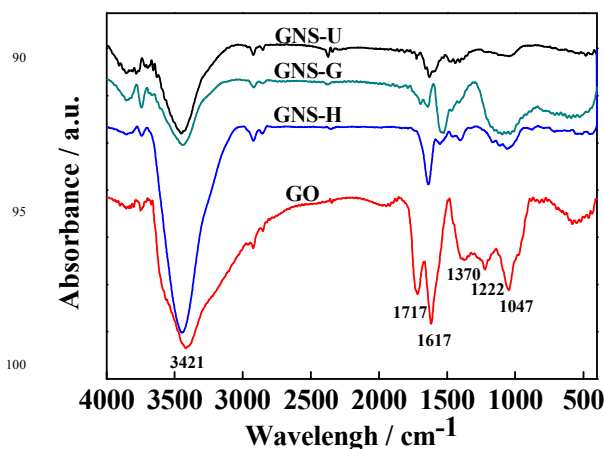


Fig.4 FTIR spectra of GO, GNS-U, GNS-G and GNS-H.

X-ray photoelectron spectroscopy analysis

XPS is one of the widely used techniques to characterize the removal of the oxygen groups in GNS. As shown in Fig.5, the $110 \text{ C}1s$ XPS spectrum of GO (Fig. 5a) clearly shows a considerable

degree of oxidation, with three different components corresponding to carbon atoms in different functional groups: the non-oxygenated ring C (C–C/C=C), epoxy and alkoxy carbon (C–O), and the carboxylate carbon (O–C=O).^{44–47} The peak of the non-oxygenated ring C (C–C) centered at 284.4 eV is attributed to bonds between sp² hybridized carbon atoms. And two peaks located at 286.6 and 288.0 eV are assigned to the epoxy and alkoxy carbon (C–O) and the carboxylate carbon (O–C=O), respectively. After its reduction with hydrazine, urea and glucose, the C1s XPS spectra of the GNS samples (Fig. 5b, 5c and 5d) all exhibit these three types of carbon. However, compared to that of GO, the absorbance band intensities of the epoxy and alkoxy carbon (C–O) and the carboxylate carbon (O–C=O) for the GNS samples all decrease significantly, indicating the removal the oxygen-containing functional groups after the reduction.

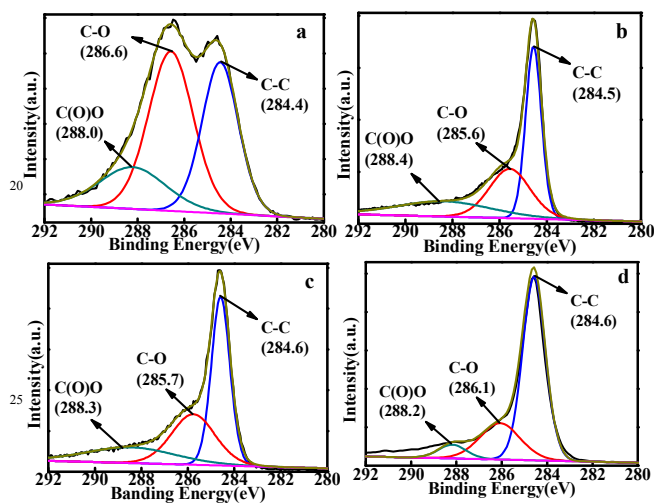


Fig. 5 C1s XPS spectra of (a) GO, (b) GNS-H, (c) GNS-U and (d) GNS-G.

Table 1 Comparison of O/C atomic ratio between GO, GNS-U, GNS-G and GNS-H.

sample	Relative C (At%)	Relative O (At%)	O/C atomic ratio
GO	69.18	30.82	0.446
GNS-U	87.86	12.14	0.138
GNS-G	89.48	10.52	0.118
GNS-H	90.11	9.89	0.110

The O/C ratio of the GO sample is 0.446 (Table 1), indicating a strong oxidation by using the modified Hummer method. After reduction, the O/C atomic ratio decreases from 0.446 (for GO) to 0.138 (for GNS-U), 0.118 (for GNS-G) and 0.110 (for GNS-H), respectively, indicating the efficient removal of oxygen functional groups.^{44, 48–49} In contrast, the O/C ratio of GNS-H (0.110) is lower than that of GNS-U and GNS-G, demonstrating that the reduction degree was in the order of hydrazine > glucose > urea. The XPS results are consistent with the Raman and IR spectra analysis.

In order to further investigate the interactions between GNS and

Ru(phen)₃Cl₂, XPS spectra analysis of the GNS samples and GNS/Ru(phen)₃Cl₂ (Ru) were also done as shown in Fig. S2. The C1s XPS spectra of the GNS samples all display a peak with binding energy (BE) of about 284.7 eV, which was assigned to C1s. As for the GNS/Ru samples, apart from the peak of C1s, the Ru3d components (Ru3d_{5/2} at 281.2 eV) can be also observed, suggesting the interaction between Ru(phen)₃Cl₂ and GNS.^{50–52} In particular, the peak of Ru 3d_{3/2} were buried under the main C1s peak.⁵²

UV-Vis and Luminescence spectra analysis

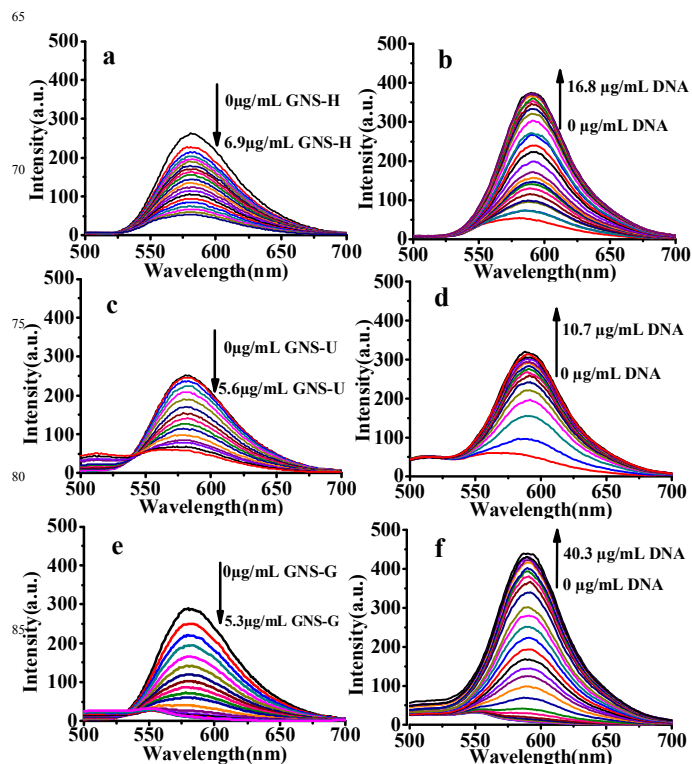


Fig. 6 Luminescence spectra of Ru(phen)₃Cl₂ in aqueous solution (a, c, e) upon addition of different concentrations of GNS-H, GNS-U, GNS-G, respectively; and (b, d, f) upon addition of different concentration of CT DNA in the presence of a certain concentration of GNS (6.9 μg/mL GNS-H, 5.6 μg/mL GNS-U, 5.3 μg/mL GNS-G), Ex=464 nm.

The UV-vis absorption spectra of the GNS samples and GNS/Ru(phen)₃Cl₂ (Ru) were shown in Fig. S3. As shown in Fig. S3, the UV-vis absorption spectra of the GNS samples in aqueous solution revealed the absorption bands at 260 nm for GNS-U, 264 nm for GNS-G, and 266 nm for GNS-H. The UV-vis spectrum of GO exhibits an absorption band at about 230 nm,¹⁶ while the absorption peak of the GNS samples all red shifted from 230 to 260–266 nm, indicating the deoxygenation of the GO and the electronic conjugation within the graphene sheets is restored after reduction with different reducing agents.⁵³ In comparison, much greater red shifts are seen in this case of GNS-H than that of GNS-G and GNS-U, and the optical absorption of the GNS-H samples was the higher than that of the equal concentration of GNS-G and GNS-U, demonstrating the highest

degree of reduction of GNS-H.^{16, 53-54} The results are consistent with the Raman, IR spectra and XPS analysis. As for the GNS/Ru(phen)₃Cl₂ samples, apart from the absorption peaks of GNS at about 260~266 nm, there was also a new absorption peaks at about 222~226 nm, corresponding to the characteristic absorption of Ru(phen)₃Cl₂. Meanwhile, The absorption spectrum of GNS/Ru(phen)₃Cl₂ samples at about 222~226 nm slightly red-shifted compared with Ru(phen)₃Cl₂ at 221 nm, indicating the interaction between Ru(phen)₃Cl₂ and GNS.⁵⁵

The luminescence spectra of Ru(phen)₃Cl₂ (0.49 μM) in aqueous solution upon addition of different concentrations of the GNS samples are shown in Fig. 6. When the GNS samples were added gradually into Ru(phen)₃Cl₂ in aqueous solution, the luminescence intensity of Ru(phen)₃Cl₂ all systematically decreases as the GNS concentration increased (Fig. 6a, 6c, 6e), suggesting that strong π-π stacking interaction and electrostatic interaction existed between GNS samples and Ru(phen)₃Cl₂. When the concentration of GNS increases to a certain value, the luminescence intensity of Ru(phen)₃Cl₂ doesn't change any further. This means that no free Ru(phen)₃Cl₂ is left in the solution at this point. Among the GNS samples, GNS-G exhibits the most pronounced quenching efficiency (Fig. 6e), suggesting much stronger interactions existed between GNS-G and Ru(phen)₃Cl₂. Then CT DNA was added gradually into the above mentioned solutions. Along with the addition of CT DNA, the luminescence intensities of the above three system with GNS-H, GNS-U and GNS-G were all increased gradually as shown in Fig. 6b, 6d and 6f, respectively. After a certain concentration of DNA was added into the above mentioned system, the luminescence intensity was all fully recovered. The reason is that after being encountered with CT DNA, Ru(phen)₃Cl₂ was released from GNS and interacted with CT DNA immediately, leading to a luminescence recovery of Ru(phen)₃Cl₂.^{26, 28} By comparison, the luminescence intensity of GNS-G was increased by 49-fold (Fig. S2c), which is far beyond that of GNS-H (only 7 times increasing as shown in Fig. S4a) and GNS-U (only 6 times increasing as shown in Fig. S4b).

As shown in Fig. S5a, Ru(phen)₃Cl₂ alone exhibited bright red luminescence under UV irradiation (Fig. S5a). When the corresponding GNS samples were added into Ru(phen)₃Cl₂, the red luminescence of the Ru(phen)₃Cl₂ was significantly quenched (Fig. S5b, S5c, S5d). Among the GNS samples, GNS-H exhibits the most pronounced quenching efficiency, and GNS-G was the second, then GNS-U. The result is consistent with the luminescence response as shown in Fig 6a, 6c and 6e. The blue luminescence was emitted by GNS-G itself, which is consistent with the literatures.⁵⁶⁻⁵⁷ After a certain concentration of DNA was added into the above mentioned system, the red luminescence was all recovered (Fig. S5e, S5f, S5g), which is consistent with the luminescence spectra analysis as shown in Fig. 6b, 6d and 6f. The reason is that after being encountered with CT DNA, Ru(phen)₃Cl₂ was released from GNS and interacted with CT DNA immediately, leading to a luminescence recovery of Ru(phen)₃Cl₂.

By comparison, the luminescence response of GNS-G (Fig. 7) shows the best linear correlation to the DNA added over the wide concentration range from 5.4 to 35.4 μg/mL, with a correlation coefficient of 0.9971. The detection limit (3σ/k method)⁵⁸ was

3.62×10^{-9} g/mL, which is lower than the literature.⁵⁹ It indicates that the GNS-G sample prepared with glucose can be employed as a carrier of Ru(phen)₃Cl₂ sensor to selective discriminate DNA. The results indicated that although the GNS samples prepared with different reductants can effectively quench the emission of the Ru(phen)₃Cl₂ sensor. After addition of a certain amount of DNA into the three systems, the luminescence intensity was all fully recovered. By comparison, the luminescence response of GNS-G prepared with glucose shows the best linear correlation to the DNA added. Therefore, the reduction degree of GNS is just one of the main factors on the sensing performance. The reason why GNS-G shows the strongest variation in luminescence intensity may be its better dispersion, better biocompatible property, better exfoliation and minimum restacking.^{16, 60}

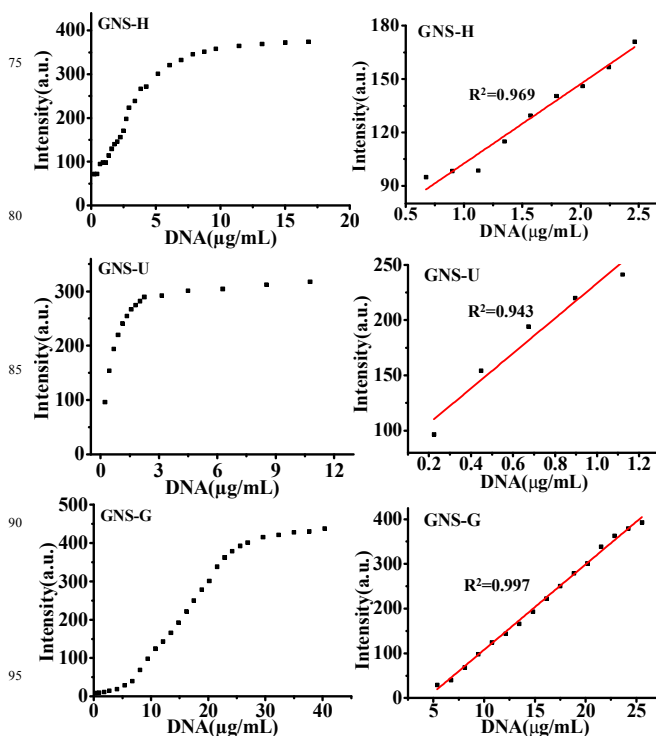


Fig.7 A calibration curve of GNS-H, GNS-U and GNS-G between the luminescence change at 590 nm and DNA added.

Conclusions

Herein, a serial of GNS were fabricated using different reducing agents, such as hydrazine, glucose and urea. The reduction degrees and properties of the obtained GNS samples were systematically investigated by X-ray diffractometer, Raman spectra, IR spectra and X-ray photoelectron spectroscopy. The results indicated that the reduction degree with hydrazine was the highest. And glucose was the second, then urea. Therefore, reducing agents plays an important role in the bulk fabrication of high quality graphene. The GNS samples were all employed as a carrier of Ru(phen)₃Cl₂ sensor to discriminate DNA. It is found that all the GNS samples can effectively quench the emission of the Ru(phen)₃Cl₂ sensor. After the addition of a certain amount of DNA into the three systems, the luminescence intensity was all

fully recovered. By comparison, the luminescence response of GNS-G prepared with glucose shows the best linear correlation to the DNA added, with a detection limit of 3.62×10^{-9} g/mL, indicating GNS-G can be employed as a good carrier of

$\text{Ru}(\text{phen})_3\text{Cl}_2$ to discriminate DNA.

In this work, the reduction degrees and properties of GNS prepared with different reducing agents were firstly systematically studied. And the feasible applications of GNS prepared with different reducing agents as a carrier of luminescent sensor were also systematically studied. It is believed that this work would advance the research of bulk fabrication of high quality graphene and the specific applications in luminescent sensor of the graphene-based functional materials in the future.

Acknowledgments

This work was supported by the National Natural Science Foundation of China (No. 201205095), the Scientific Research Foundation of Northwest A&F University (Z109021115, Z111021103 and Z111021107), the Fundamental Research Funds for the Central Universities (Z109021204), Shaanxi Province Science and Technology (No. 2013K12-03-23), State Key Laboratory of Chemo/Biosensing and Chemometrics, Hunan University (No. 2013005), Open Project of Key Laboratory of Applied Surface and Colloid Chemistry (No. 2014012).

Notes and references

College of Science, Northwest A&F University, Yangling, Shaanxi, 712100, P. R. China. Fax: +86-29-87082832; Tel: +86-29-87092226; E-mail: sunsg@nwsuaf.edu.cn

† Electronic Supplementary Information (ESI) available: [The structures of $\text{Ru}(\text{phen})_3\text{Cl}_2$; Cls XPS spectra of the GNS samples and GNS/ $\text{Ru}(\text{phen})_3\text{Cl}_2$ (Ru); UV-vis absorption spectra of the GNS samples and GNS/Ru. Luminescence response of the $\text{Ru}(\text{phen})_3\text{Cl}_2$ sensor upon addition of different concentration of CT DNA in the presence of GNS; Optical image of $\text{Ru}(\text{phen})_3\text{Cl}_2$ (Ru), Ru+GNS and Ru+GNS+DNA]. See DOI: 10.1039/b000000x/

- X. Y. Dong, L. Wang, D. Wang, C. Li and J. Jin, *Langmuir*, 2012, **28**, 293.
- C. N. R. Rao, A. K. Sood, K. S. Subrahmanyam and A. Govindaraj, *Angew. Chem. Int. Ed.*, 2009, **48**, 7752.
- Z. C. Xing, Q. X. Chu, X. B. Ren, J. Q. Tian, A. M. Asiri, K. A. Alamry, A. O. Al-Youbi, X. P. Sun. *Electrochem. Commun.*, 2013, **32**, 9.
- H. Y. Li, S. Liu, J. Q. Tian, L. Wang, W. B. Lu, Y. L. Luo, A. M. Asiri, A. O. Al-Youbi and X. P. Sun. *ChemCatChem*. 2012, **4**, 1079.
- Y. W. Zhang, J. Q. Tian, H. Y. Li, L. Wang, X. Y. Qin, A. M. Asiri, A. O. Al-Youbi and X. P. Sun. *Langmuir* 2012, **28**, 12893.
- D. Chen, L. H. Tang and J. H. Li, *Chem. Soc. Rev.*, 2010, **39**, 3157.
- Y. X. Liu, X. C. Dong and P. Chen, *Chem. Soc. Rev.*, 2012, **41**, 2283.
- A. Marinkas, F. Arena, J. Mitzel, G. M. Prinz, A. Heinzl, V. Peinecke and H. Natter, *Carbon*, 2013, **58**, 139.
- G. Q. Xu, P. W. Xu, D. J. Shi and M. Q. Chen, *RSC Adv.*, 2014, **4**, 28807.
- W. H. Shang, X. Y. Zhang, M. Zhang, Z. T. Fan, Y. Sun, M. Han and L. Z. Fan, *Nanoscale*, 2014, **6**, 5799.
- S. Liu, J. Q. Tian, L. Wang and X. P. Sun. *Carbon* 2011, **49**, 3158.
- S. Liu, J. Q. Tian, L. Wang, H. L. Li, Y. W. Zhang and X. P. Sun. *Macromolecules* 2010, **43**, 10078.
- Z. J. Fan, W. Kai, J. Yan, T. Wei, L. J. Zhi, J. Feng, Y. M. Ren, L. P. Song and F. Wei, *ACS Nano.*, 2011, **5**, 191.

- L. J. Deng.; G. Zhu, J. F. Wang, L. P. Kang, Z. H. Liu, Z. P. Yang and Z. L. Wang, *J. Power Sources*, 2011, **196**, 10782.
- L. J. Zhang, X. G. Zhang, L. F. Shen, B. Gao, L. Hao, X. J. Lu, F. Zhang, B. Ding and C. Z. Yuan, *J. Power Sources*, 2012, **199**, 395.
- C. Z. Zhu, S. J. Guo, Y. X. Fang and S. J. Dong, *ACS nano.*, 2010, **4**, 2429.
- M. Quintana, E. Vazquez and M. Prato, *Acc. Chem. Res.*, 2013, **46**, 138.
- F. X. Xiao, J. W. Miao and B. Liu, *J. Am. Chem. Soc.*, 2014, **136**, 1559.
- H. L. Li, Y. W. Zhang, L. Wang, J. Q. Tian and X. P. Sun. *Chem. Commun.*, 2011, **47**, 961.
- H. L. Li, J. Q. Tian, L. Wang, Y. W. Zhang and X. P. Sun. *J. Mater. Chem.*, 2011, **21**, 824.
- S. Liu, H. L. Li, L. Wang, J. Q. Tian and X. P. Sun. *J. Mater. Chem.*, 2011, **21**, 339.
- H. L. Li, Y. W. Zhang, T. S. Wu, S. Liu, L. Wang and X. P. Sun. *J. Mater. Chem.*, 2011, **21**, 4663.
- H. L. Li, Y. W. Zhang, Y. L. Luo and X. P. Sun. *Small* 2011, **7**, 1562.
- B. J. Hong, O. C. Compton, Z. An, I. Eryazici and S. T. Nguyen, *ACS Nano.*, 2012, **6**, 63.
- J. Kim, L. J. Cote, F. Kim and J. Huang, *J. Am. Chem. Soc.*, 2010, **132**, 260.
- A. B. Tossi and J. M. Kelly, *Photochem. Photobiol.*, 1989, **49**, 545.
- C. Hiort, B. Nordén and A. Rodger, *J. Am. Chem. Soc.*, 1990, **112**, 1971.
- D. Z. M. Coggan, I. S. Haworth, P. J. Bates, A. Robinson and A. Rodger, *Inorg. Chem.*, 1999, **38**, 4486.
- H. J. Li, F. Y. Liu, S. G. Sun, J. Y. Wang, Z. Y. Li, D. Z. Mu, B. Qiao and X. J. Peng. *J. Mater. Chem. B*, 2013, **1**, 4146.
- P. A. Lay, A. M. Sargeson, H. Taube, M. H. Chou and C. Creutz, *Inorg. Synth.*, 1986, **24**, 291.
- W. S. Hummers and R. E. Offeman, *J. Am. Chem. Soc.*, 1958, **80**, 1339.
- Z. H. Liu, Z. M. Wang, X. J. Yang and K. Ooi, *Langmuir*, 2002, **18**, 4926.
- X. Wang, S. Zhou, W. Y. Xing, B. Yu, X. M. Feng, L. Song and Y. Hu, *J. Mater. Chem. A*, 2013, **1**, 4383.
- Y. Y. Shao, J. Wang, M. Engelhard, C. M. Wang and Y. H. Lin. *J. Mater. Chem.* 2010, **20**, 743.
- Y. C. Si and E. T. Samulski. *Nano Lett.* 2008, **8**, 1679.
- F. Tuinstra and J. L. Koenig, *J. Chem. Phys.*, 1970, **53**, 1126.
- A. C. Ferrari and J. Robertson, *Phys. Rev. B*, 2000, **61**, 14095.
- C. Navarro, R. T. Weitz, A. M. Bittner, M. Scolari, A. Mews, M. Burghard and K. Kern, *Nano. Lett.*, 2009, **9**, 2206.
- S. Stankovich, A. A. Dikin, R. D. Piner, K. A. Kohlhaas, A. Kleinhammes, Y. Y. Jia, Y. Wu, S. T. Nguyen, R. S. Ruoff, *Carbon*, 2007, **45**, 1558.
- G. X. Wang, J. Yang, J. S. Park, X. L. Gou, B. Wang, H. Liu and J. Yao, *J. Phys. Chem. C*, 2008, **112**, 8192.
- G. Q. Luo, X. J. Jiang, M. J. Li, Q. Shen, L. M. Zhang and H. G. Yu, *ACS Appl. Mater. Interfaces*, 2013, **5**, 2161.
- Y. Li, N. Q. Zhao, C. S. Shi, E. Z. Liu, and C. N. He. *J. Phys. Chem. C*, 2012, **116**, 25226.
- W. Zhang, Y. X. Zhang, Y. Tian, Z. Y. Yang, Q. Q. Xiao, X. Guo, L. Jing, Y. F. Zhao, Y. M. Yan, J. S. Feng and K. N. Sun. *ACS Appl. Mater. Interfaces* 2014, **6**, 2248.
- K. Liu, L. Chen, Y. Chen, J. L. Wu, W. Y. Zhang, F. Chen and Q. Fu. *J. Mater. Chem.*, 2011, **21**, 8612.
- D. Briggs and G. Beamson, *The Scienta ESCA300 Database*. New York: John Wiley and Sons, 1992.
- X. Wang, S. Zhou, W. Y. Xing, B. Yu, X. M. Feng, L. Song and Y. Hu. *J. Mater. Chem. A*, 2013, **1**, 4383.
- X. J. Zhou, J. J. Zhang, H. X. Wu, H. J. Yang, J. Y. Zhang and S. W. Guo. *J. Phys. Chem. C*, 2011, **115**, 11957.
- Y. W. Zhu, M. D. Stoller, W. W. Cai, A. Velamakanni, R. D. Piner, D. Chen, and R. S. Ruoff. *ACS Nano.*, 2010, **4**, 1227.
- D. Y. Wan, C. Y. Yang, T. Q. Lin, Y. F. Tang, M. Zhou, Y. J. Zhong, F. Q. Huang and J. H. Lin. *ACS Nano.*, 2012, **6**, 9068.
- U. Unal, Y. Matsumoto, N. Tanaka, Y. Kimura and N. Tamoto. *J. Phys. Chem. B* 2003, **107**, 12680.

- 51 Y. V. Larichev. *J. Phys. Chem. C* 2008, **112**, 14776.
- 52 L. M. Martínez-Prieto, S. Carencó, C. H. Wu, E. Bonnefille, S. Axnanda, Z. Liu, P. F. Fazzini, K. Philippot, M. Salmeron and B. Chaudret. *ACS Catal.* 2014, **4**, 3160.
- 53 L. X. Lin and S. W. Zhang. *J. Mater. Chem.*, 2012, **22**, 14385.
- 54 V. H. Pham, H. D. Pham, T. T. Dang, S. H. Hur, E. J. Kim, B. S. Kong, S. Kim and J. S. Chung. *J. Mater. Chem.*, 2012, **22**, 10530.
- 55 G. F. Gui, Y. Zhuo, Y.Q. Chai, N. Liao, M. Zhao, J. Han, Y. Xiang and R. Yuan. *RSC Adv.*, 2014, **4**, 1955.
- 56 Y. Q. Dong, G. L. Li, N. Zhou, R. X. Wang, Y. W. Chi and G. N. Chen. *Anal. Chem.* 2012, **84**, 8378.
- 57 J. H. Shen, Y. H. Zhu, C. Chen, X. L. Yang and C. Z. Li. *Chem. Commun.*, 2011, **47**, 2580.
- 58 X. B. Zhang, Z. D. Wang, H. Xing, Y. Xiang and Y. Lu, *Anal. Chem.*, 2010, **82**, 5005.
- 59 L. P. Wang, C. C. Guo, B. Fu and L. Wang, *J. Agric. Food Chem.*, 2011, **59**, 1607.
- 60 O. Akhavan, E. Ghaderi, S. Aghayee, Y. Fereydoonia and A. Talebi. *J. Mater. Chem.*, 2012, **22**, 13773.